

A. FERNÁNDEZ<sup>1,✉</sup>  
A. VERHOEF<sup>1</sup>  
V. PERVAK<sup>2,3</sup>  
G. LERMANN<sup>4</sup>  
F. KRAUSZ<sup>2,3</sup>  
A. APOLONSKI<sup>2,3,5</sup>

# Generation of 60-nJ sub-40-fs pulses at 70 MHz repetition rate from a Ti:sapphire chirped pulse-oscillator

<sup>1</sup> Institut für Photonik, Technische Universität Wien, Gusshausstrasse 27/387, 1040 Wien, Austria  
<sup>2</sup> Max-Planck-Intitut für Quantenoptik, Hans-Kopfermann-Strasse 1, 85748 Garching, Germany  
<sup>3</sup> Department für Physik, Ludwig-Maximilians-Universität München, Am Coulombwall 1, 85748 Garching, Germany  
<sup>4</sup> Coherent Germany, Dieselstraße 5b, 64807 Dieburg, Germany  
<sup>5</sup> Institute of Automation and Electrometry, RAS, 630090 Novosibirsk, Russia

Received: 13 March 2007

Published online: 25 April 2007 • © Springer-Verlag 2007

**ABSTRACT** We have studied the influence of the intracavity dispersion on the mode-locking characteristics of pure-Kerr-lens mode-locked Ti:sapphire chirped-pulse oscillators. Using the results of this study, we have built chirped-pulse oscillators that can be mode-locked when pumped with the highest pump powers commercially available at 532 nm. We generated 62 nJ pulses at 70 MHz repetition rate, with a Fourier limited duration of 33 fs.

**PACS** 42.60.Fc; 42.60.Lh; 42.65.Re

## 1 Introduction

High resolution spectroscopy with frequency combs is a well established technique that allowed to do high precision measurements ranging from infrared wavelength to ultraviolet wavelengths. However, extension of this technique to the extreme ultraviolet requires frequency combs with substantially more energy than conventionally available. Recently generation of high harmonic radiation with a near-infrared frequency comb in a femtosecond enhancement cavity was demonstrated [1, 2]. The master oscillator for the enhancement cavity in these experiments were conventional oscillators delivering < 10 nJ pulses at a repetition rate around 100 MHz. Increasing the pulse energy from the master oscillator will substantially enhance the results achievable with this technique, especially to improve the conversion efficiency of the harmonic radiation, and to extend the frequency comb to even shorter wavelengths.

With  $\leq 50$  nJ pulses from extended cavity oscillators successful writing of

waveguides in different transparent materials was demonstrated [3–5]. In recent experiments a new kind of waveguide consisting of a chain of so-called ‘pearl structures’ [4] has been created by applying 30-fs pulses with an energy below 50 nJ at a repetition rate of 11 MHz. This application will greatly benefit as well from the availability of comparable high-energy pulses at higher repetition rates. More thermal effects can be utilized and structures can be written at greater speeds than with sources available up to now.

Previous demonstrations of high-energy pulses from oscillators focused at increasing the pulse energy by decreasing the oscillator repetition rate, in order to overcome the occurrence of instabilities such as multipulsing and cw generation due to excess nonlinearities in the laser medium as the pulse energy increases [6–9].

We demonstrate another approach to generate pulses with moderate energy with pure-Kerr-lens mode-locked Ti:sapphire chirped-pulse oscillators. We generated 54 nJ pulses at 80 MHz repetition rate and 62 nJ pulses at

70 MHz repetition rate, compressible to less than 40 fs. For this, we have investigated the influence of intra-cavity dispersion on the mode-locked operation of such systems. In oscillators operating with net negative intracavity dispersion, mode-locked operation can not be maintained at high pump powers due to excess nonlinearities in the laser medium. We have optimized the exact shape of the intracavity dispersion of our oscillator working with net positive intracavity dispersion to allow stable mode-locked operation even at high pump powers.

## 2 Design considerations for chirped pulse oscillators

### 2.1 Starting of mode-locked operation

There are only a few but no detailed studies on the dispersion effects on the spectral and temporal characteristics of pure-Kerr-lens mode-locked oscillators operating with net positive dispersion. Most of the few studies on this kind of systems were carried out by using a saturable Bragg reflector (SBR) to assist starting of mode-locked operation [9] or by starting the oscillator while having net negative intracavity dispersion and then increasing the intracavity dispersion until it reaches net positive values by insertion of intracavity dispersive elements such as prisms [10] or wedges.

SBRs have the disadvantages that until now the maximal spectral width demonstrated is around 40 nm [7, 9], that they introduce high intracavity losses in Ti:sapphire oscillators equipped with them, and are subject to degradation effects.

✉ Fax: +43 158801 38799, E-mail: almadelc@mail.zserv.tuwien.ac.at

## 2.2 Maximal spectral width achievable

Theoretical simulations have predicted that in Ti:sapphire oscillators with net positive dispersion, and an appropriate form of the intracavity dispersion curve, pulses with a spectral width exceeding 100 nm can be achieved [11]. A careful design of the intracavity dispersion, with moderate fourth-order dispersion (FOD) (yielding a dispersion minimum around the central wavelength) provides the most stable mode-locked operation with the broadest spectral width. Theoretical calculations predict M-shaped output spectra for a net intracavity dispersion close to zero in the presence of positive FOD. For increasing net dispersion, the predicted output spectra change to flat-top (or  $\Pi$ -shape) and then parabolic-like spectra, with decreasing spectral width.

## 2.3 Influence of the shape of the intracavity dispersion

Experimentally, we have found that the ability to start mode-locked operation in an oscillator with net positive dispersion is strongly dependent on the shape of the intracavity dispersion. The maximum output power in mode-locked operation depends on this, too. The latter can be expressed as well in other terms, namely that the shape of the intracavity dispersion determines the position in the stability range where mode-locked operation can be started. In practise, the mirror M1 (as seen in Fig. 1) is moved closer to the Ti:sapphire crystal in order to reach the point in the stability range where mode-locked operation can be started.

With the ABCD-matrix formalism, two sets of distances between the mirrors M1 and M2 can be found where stable lasing can be obtained in the cavity, the so-called stability zones. The cavity shown in Fig. 1 is operated in the stability region with the largest separation between the mirrors M1 and M2, the outer stability zone. For both stability regions, a maximum output power in cw operation can be found for a certain mirror separation, and when the mirror separation is changed from this position, the output power decreases.

For Kerr-lens mode-locked oscillators operating with net negative intracavity dispersion, the position of the

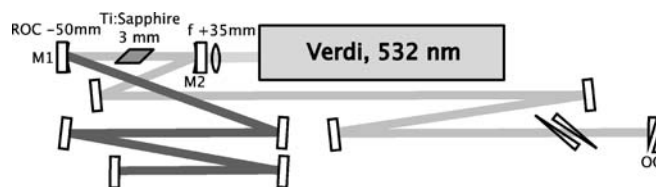


**FIGURE 1** Schematic of the oscillator used in our experiments. The radius of curvature (ROC) of the mirrors M1 and M2 is  $-50$  mm. The optical path length of the Brewster-cut Ti:sapphire crystal is 3 mm. The insertion of the intracavity wedges can be varied to change the net intracavity dispersion. The mirror M1 can be moved to change the position in the stability range, in order to allow starting of mode-locked operation. We used a 29% output coupler when the oscillator was pumped with an 18-W Verdi

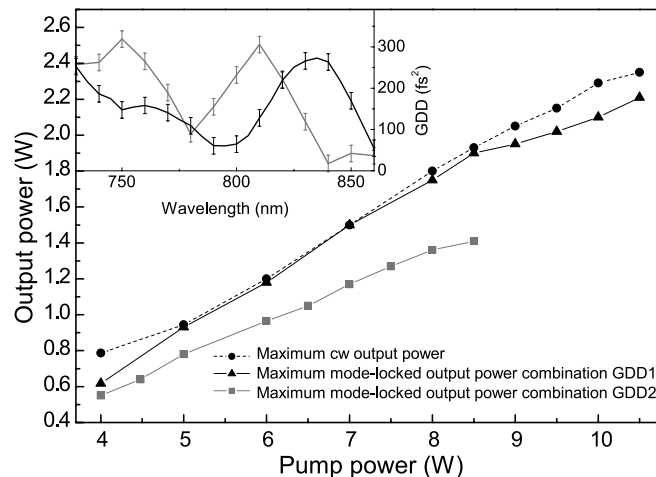


**FIGURE 2** Maximum output power versus pump power for two different mirror combinations (GDD1, black, and GDD2, gray) in mode-locked operation and in cw operation (dashed black). The maximum output power in cw operation was the same for both mirror combinations. *Inset*: Total intracavity dispersion versus wavelength for both mirror combinations. The net dispersion can be varied with the intracavity wedges, and can therefore be considered the same for both mirror combinations. The accuracy of the given GDD values is mainly limited by the accuracy of the GDD measurements of the individual mirrors

mirror M1 where mode-locked operation can be started and maintained is generally substantially closer to the laser crystal than that for operation with maximum cw power. This results in a substantially lower maximum output power in mode-locked operation than in cw operation. For Kerr-lens mode-locked oscillators operating with net positive intracavity dispersion, the position of the mirror M1 where mode-locked operation can be started can be much closer to the position where maximum cw output power is achieved. This results in much higher output power in mode-locked operation, depending on the shape of the intracavity dispersion, as we have observed.

In Fig. 2 the maximum output power versus pump power in mode-locked operation and cw operation is shown for two different mirror combinations, and thus two different shapes of the intracavity dispersion. The maximum cw output power with both mirror combinations was the same, showing that

the difference in mirror losses for both combinations is negligible. The oscillator with dispersion curve GDD1 can work in mode-locked operation at much higher pump powers than the oscillator with dispersion curve GDD2. The dispersion curve GDD1 has a dispersion minimum closer to the gain maximum of Ti:sapphire, and appears more smooth around the dispersion minimum than the dispersion curve GDD2. It can be clearly seen that the curve GDD1 has a moderate amount of positive FOD around the gain maximum. By taking twice the derivative of the curve GDD1, we calculate an FOD of  $14\,000\text{ fs}^4$ . This agrees with the theoretical prediction that mode-locked operation is more stable in the presence of moderate positive FOD [11].

## 2.4 Dependence of the spectral width on intracavity energy and dispersion

Another important observation is that when the intracavity disper-

sion is kept constant, and the intracavity energy is increased (by increasing the pump power), the spectral width increases, as can be seen in Fig. 3. For constant intracavity energy, the spectral width increases for decreasing net intracavity dispersion, in accordance to theoretical predictions [11]. From these two observations, it seems that increasing the intracavity energy tends to decrease the net intracavity dispersion ‘felt’ by the pulse. The observed spectral width of about 100 nm at a pump power of 10 W is, to our knowledge, the broadest bandwidth observed for this type of oscillators until now.

In order to build an oscillator that can deliver a broad spectrum that can be used at low and high pump powers, a means to change the net intracavity dispersion is necessary. We include a pair of intracavity wedges in our setup to allow tuning of the net intracavity dispersion. The wedges allow only tuning of the intracavity dispersion over a limited range (about  $60 \text{ fs}^2$ ), and thus to achieve comparable spectral width over a limited range of pump powers (for example from 8 to 10 W). For broader tunability of the intracavity dispersion, a pair of intracavity Brewster-cut prisms may be added, for example as is described in [8].

### 3 Chirped-pulse oscillator with high-energy 30-fs output pulses

On the basis of the above considerations, we designed chirped-pulse oscillators to be pumped with an 18-W Verdi (Coherent GmbH). A schematic of our setup is shown in Fig. 1.

The first system we built delivered the best output parameters at around 10 W of pump power. The output power was 2.3 W at a repetition rate of 70 MHz, resulting in a pulse energy of 33 nJ. In Fig. 4 the output spectrum and the intracavity dispersion are shown. The output pulses were compressed using a LAK21 prism compressor in a double-pass configuration, and the pulse duration was measured with an interferometric second-harmonic autocorrelator.

In Fig. 5, we show an autocorrelation trace of the compressed output pulses from our system pumped with 10 W, yielding a pulse duration of  $30 \pm 1 \text{ fs}$ . The measured pulse duration is slightly more than the Fourier-limited

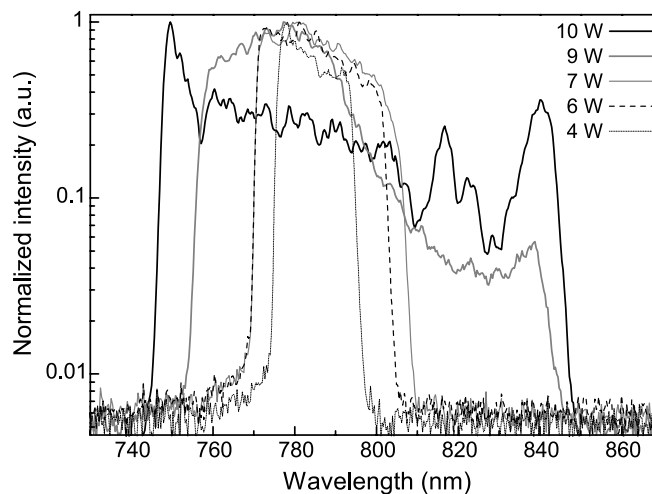


**FIGURE 3** Output spectrum for different pump powers at constant intracavity dispersion. The increase of spectral bandwidth with increasing pump power can be clearly observed. At 10 W pump power, a spectral width of about 100 nm is observed, the broadest reported so far for oscillators operating with net positive intracavity dispersion

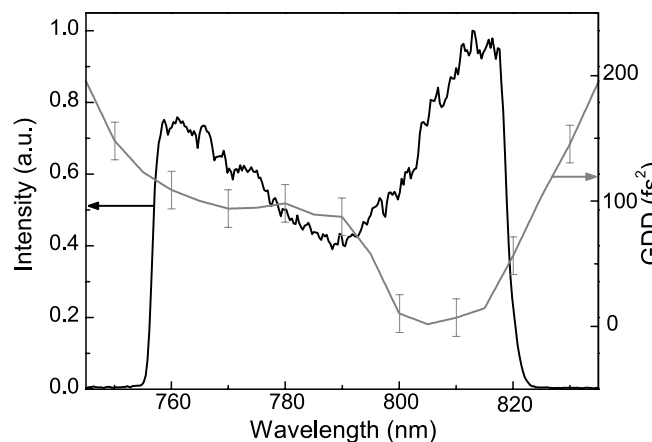


**FIGURE 4** Intracavity dispersion and output spectrum of the oscillator at a repetition rate of 70 MHz at a pump power of 10 W. The output power of 2.3 W corresponds to an output pulse energy of 33 nJ

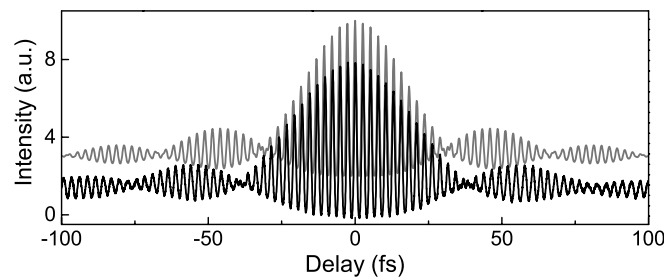


**FIGURE 5** Autocorrelation trace of the compressed output pulses from the 70 MHz oscillator with an average output power of 2.3 W. The vertically offset gray trace is calculated from the measured spectrum with flat phase assumed (corresponding to the Fourier-limited duration of 27 fs). We fitted the duration of the measured autocorrelation trace to be  $30 \pm 1 \text{ fs}$

duration of 27 fs. The discrepancy between the Fourier-limited duration and the measured duration can be well explained with the theoretically predicted chirp of the output pulses [11], the higher-order components of which can not be compressed with the prism-compressor.

From the 97 cm apex-to-apex separation of the prisms of the compressor, we derive a chirp on the output pulses from the oscillator of  $3177 \text{ fs}^2$ . With this chirp, the pulse duration inside the laser cavity can be calculated to be 610 fs.

We have built a second system with a different intracavity dispersion curve,

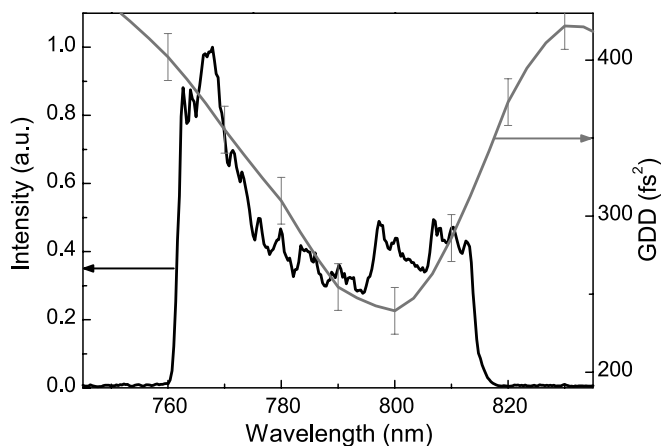


**FIGURE 6** Intracavity dispersion and output spectrum of the oscillator at a repetition rate of 70 MHz at a pump power of 18.5 W. The output power of 4.3 W corresponds to an output pulse energy of 62 nJ. The Fourier limited duration of the pulses is 33 fs

that allowed stable mode-locked operation at a pump power of 18.5 W. In Fig. 6 we show the output spectrum and intracavity dispersion of the chirped-pulse oscillator at a repetition rate of 70 MHz and a pump power of 18.5 W. The uncompressed output power was 4.3 W, thus yielding an output pulse energy of 62 nJ. The Fourier limited duration of these pulses is 33 fs. When the cavity-length of the oscillator was changed to provide a repetition rate of 80 MHz, the same output power was achieved in mode-locked operation, thus yielding a pulse energy of 54 nJ.

#### 4 Conclusions

We have studied the influence of the intracavity dispersion on the mode-locking characteristics of pure Kerr-lens mode-locked Ti:sapphire

chirped-pulse oscillators. Both the shape and the net value of the intracavity dispersion are very important for the ability to start and maintain stable mode-locked operation at high pump powers. Stable mode-locked operation can be achieved with a minimum in the intracavity dispersion close to the gain maximum of Ti:sapphire, and with a smooth shape of the intracavity dispersion yielding a moderate positive FOD, in agreement with theoretical predictions [11].

As a result of this study, we have built chirped-pulse oscillators that deliver the highest possible output pulse energy at given pump powers. We characterized the output pulses from a 70 MHz chirped-pulse oscillator at a pump power of 10 W. It was possible to compress the 33-nJ pulses to almost the Fourier limited duration of 27 fs, and we determined the compressed pulse duration to be  $30 \pm 1$  fs.

We built a chirped-pulse oscillator with optimized dispersion to be pumped with the highest available power from an 18-W Verdi. Stable mode-locked operation at 80 and 70 MHz was achieved, with an average output power of 4.3 W, yielding respectively 54 and 62 nJ pulses with a Fourier limited pulse duration of 33 fs.

**ACKNOWLEDGEMENTS** The authors acknowledge helpful discussions with V. Kalashnikov, S. Naumov and G. Tempea, and thank C. Gohle and R. Graf for experimental support.

#### REFERENCES

- 1 R.J. Jones, K. Moll, M. Thorpe, J. Ye, *Phys. Rev. Lett.* **94**, 193 201 (2005)
- 2 C. Gohle, T. Udem, M. Herrmann, J. Rauschenberger, R. Holzwarth, H.A. Schuessler, F. Krausz, T.W. Hänsch, *Nature* **234**, 436 (2005)
- 3 K. Suzuki, V. Sharma, J.G. Fujimoto, E.P. Ippen, Y. Nasu, *Opt. Express* **14**, 2335 (2006)
- 4 R. Graf, A. Fernandez, M. Dubov, H. Brückner, B. Chichkov, A. Apolonski, *Appl. Phys. B* **87**, 21 (2006)
- 5 C.B. Schaffer, A. Brodeur, J.F. Garcia, E. Mazur, *Opt. Lett.* **26**, 93 (2001)
- 6 J. Soto-Crespo, N. Akhmediev, V. Afanasjev, *J. Opt. Soc. Am. B* **13**, 1439 (1996)
- 7 A.M. Kowalevicz, A.T. Zare, F.X. Kärtner, J.G. Fujimoto, S. Dewald, U. Morgner, V. Scheuer, G. Angelow, *Opt. Lett.* **28**, 1597 (2003)
- 8 A. Fernandez, T. Fuji, A. Poppe, A. Fürbach, F. Krausz, A. Apolonski, *Opt. Lett.* **29**, 1366 (2004)
- 9 S. Naumov, A. Fernandez, R. Graf, P. Dombi, F. Krausz, A. Apolonski, *New J. Phys.* **7**, 216 (2005)
- 10 B. Proctor, E. Westwig, F. Wise, *Opt. Lett.* **18**, 1654 (1993)
- 11 V.L. Kalashnikov, E. Podivilov, A. Chernykh, S. Naumov, A. Fernandez, R. Graf, A. Apolonski, *New J. Phys.* **7**, 217 (2005)